Design and Analyze of a Monolithic Square Spiral Planar Micro-Transformer

Benhadda Yamina
Department of Electrical Engineering
University of Science and Technology
Oran, Algeria
benhadda_yamina@yahoo.fr

Derkaoui Mokhtaria
National Institute of Telecommunication
Oran, Algeria
mderkaoui@inttic.dz

Mendaz Kheira
Department of Electrical Engineering
University of Centre Belhadj Bouchaib
Ain Temouchent, Algeria
kheiramendez@gmail.com

Kharbouch Hayet
Department of Electrical Engineering
University of Science and Technology
Oran, Algeria
hayet.kharbouch@gmail.com

***Abstract*—The integration of electrical components has been the subject of many researches. In this paper, we design and analyze a monolithic square spiral planar micro-transformer integrated in a converter Flyback.**
Firstly, the geometrical and electrical parameters are presented. Secondly, the efficiency of Flyback is calculated to verify the performance of the converter. The final part of this paper shows the thermal modeling, using the finite element method that allowed us to determine the operating temperature in the materials of this component.

***Keywords*—** monolithic square spiral planar micro-transformer, converter flyback, thermal

I. INTRODUCTION

Several studies demonstrated the feasibility of integrated inductors on Silicon substrates, huge research efforts have been dedicated to their analysis, design, modeling and optimization [1-4]. As a result of these efforts, the inductor performance has been noticeably improved. Conversely, integrated transformers still remain strange components and are rarely used.
In this paper we will design and analyze the integrated or monolithic micro-transformer integrated in converter Flyback. This component is the coupling of two square inductor results. The finite element method has allowed us to see the evolution of the temperature in the different parts that make up the micro-transformer in 3D.

II. PRESENTATION OF THE FLYBACK CONVERTER

We have chosen a Flyback converter (figure 1) because it is composed of a transformer. The principle of operation of the Flyback is based on the energy transfer from primary to secondary through a transformer.

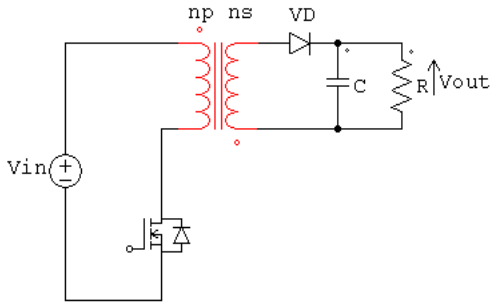

Fig. 1. Schematic of Flyback converter

The main specifications is presented in table I

TABLE I. MAIN SPECIFICATION

Parameters	Values
Input Voltage [V_{in}] (V)	14
Output voltage [V_{out}] (V)	12
Output power [P_{out}] (W)	5
Duty cycle [α] 0.5	0.5
Operation Frequency (MHz)	100

III. DIMENSIONING OF THE MICRO-TRANSFORMER

Dimensioning of the planar Micro-Transformer requires sizing the magnetic circuit and the geometrical parameters of two wading of our component, primary and secondary [5-6].
Turn ratio

$$m = \frac{\alpha}{\alpha - 1}\frac{V_{out}}{V_{in}} = 0.85 \qquad (1)$$

The primary inductance L_p is given by relation (2)

$$L_p = \frac{V_{in}^2 \alpha^2}{2 f P_{out}} \qquad (2)$$

The operation of passive transformer is based on the mutual coupling between two or more conductors, or more currently, inductors. An example of an integrated implementation it is shown in figure 2 where two inductors are intertwined in order to favor their mutual coupling.

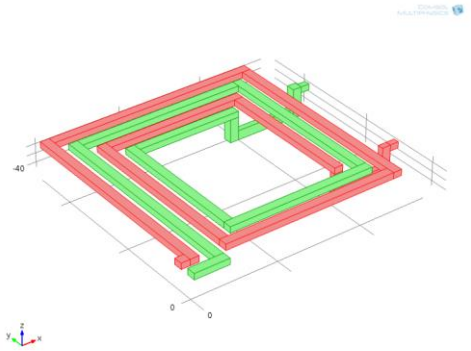

(a)

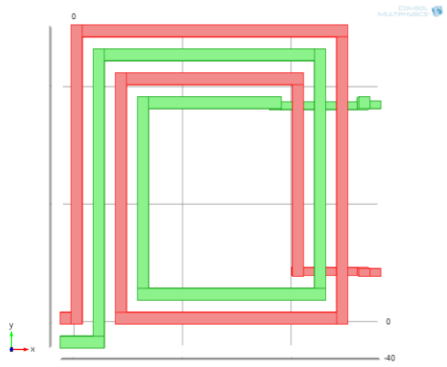

(b)

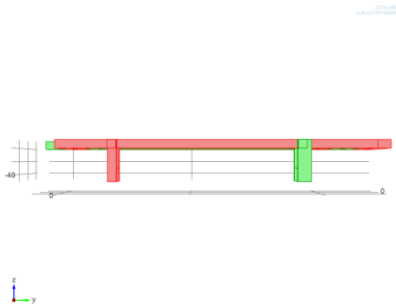

(c)

Fig. 2. Integrated planar micro-transformer , (a) general view, (b) view dessu, (c) front view

Primary and secondary turns' numbers are calculated by Mohan's [7-8] formula (3). The coefficients k_1 and k_2 are defined for each geometry. For a square micro coil spiral, k_1=2.34 and k_2=2.75.

$$n_p = \sqrt{\frac{L_p(1+k_2\rho)}{K_1\mu_0 d_{avg}}} \quad (3)$$

$$n_s = m.n_p \quad (4)$$

Where, we define the average diameter as $d_{avg} = (d_{out} + d_{in})/2$. A_m the factor's form defined as $A_m = d_{out} - d_{in} / d_{out} + d_{in}$.

We have taken the same spacing for both the primary and secondary windings, $w_p = w_s$:

$$w_p = w_s = \frac{[d_{out} - d_{in} - 2s_s(n_s - 1)]}{2n_s} \quad (5)$$

The primary and secondary spacing between conductors is expressed as follows

$$s_p = \frac{d_{out} - d_{in} - 2w_p n_p}{2(n_p - 1)} \quad (6)$$

$$s_s = \frac{d_{out} - d_{in} - 2w_s n_s}{2(n_s - 1)} \quad (7)$$

The primary and secondary length of the trace is expressed as follows

$$l_p = 4n_p[d_{out} - (n_p - 1)s_p - n_p w_p] - s_p \quad (8)$$

$$l_s = 4n_s[d_{out} - (n_s - 1)s_s - n_s w_s] - s_s \quad (9)$$

The skin thickness is defined as [9]

$$\delta = \sqrt{\frac{\rho}{\pi\mu f}} \quad (10)$$

Where ρ represent the resistivity of the conductor, $\rho = 1.7\ 10^{-8}\Omega m$ and μ its magnetic permeability. So that the current flows in the entire conductor, it is necessary that one of the following conditions is filled, $w \le 2\delta$ or $t \le 2\delta$.

Table II contains the specifications and the design results of the integrated micro-transformer.

Table II. Design results of the integrated micro-transformer

Parameter	Value
Outer diameter: d_{out}	500 µm
Inner diameter: d_{in}	450 µm
Primary turns: n_p	1.75
Secondary turns: n_s	1.25
Thickness of winding: t	13 µm
Width of primary winding: w_p	20 µm
Width of secondary winding: w_s	20 µm
Inter-spacing of primary winding: s_p	4.2 µm
Inter-spacing of secondary winding: s_s	6. 5 µm
Length of primary winding: l_p	3.2 µm
Length of secondary winding: l_s	2.8 µm

IV. ELECTRICAL MODEL

An accurate planar micro-transformer model is desired for circuit design (figure 3).

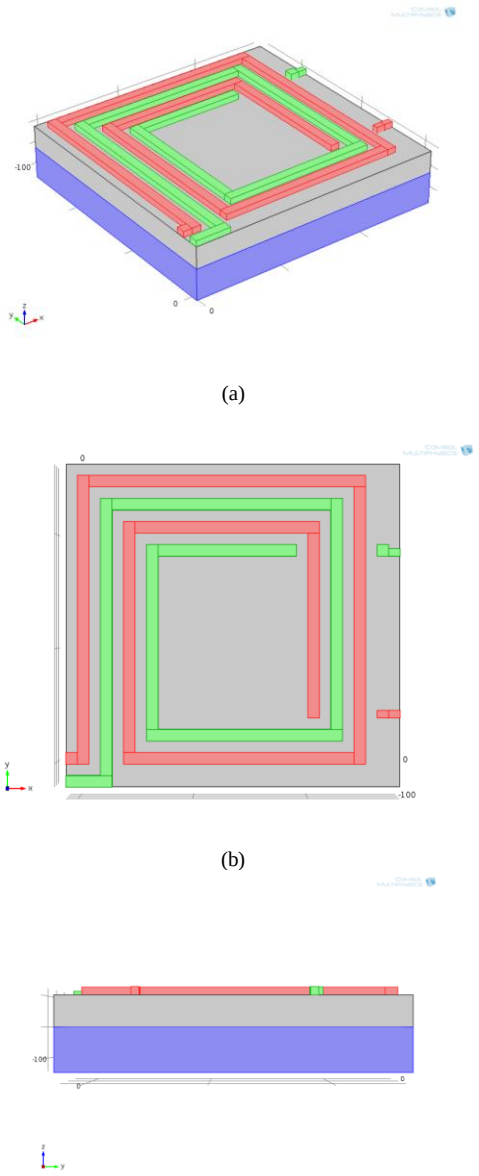

(a)

(b)

(c)

Fig. 3. Geometry of integrated micro-transformer on substrate on substrate, (a) general view, (b) view dessu, (c) front view

The equivalent electrical model of an integrated planar micro-transformer [10] is shown in Figure 4.

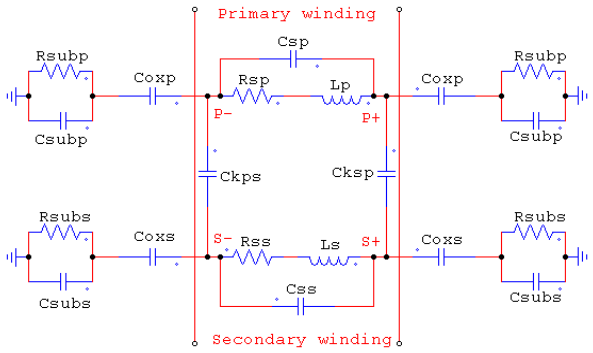

Fig. 4. Equivalent circuit of an integrated planar micro-transformer

1. Serial resistance R_{sp} and R_{ss} of the primary and secondary

$$R_{sp} = \frac{\rho_{cu} l_p}{w_p t} \quad (11)$$

$$R_{ss} = \frac{\rho_{cu} l_s}{w_s t} \quad (12)$$

2. Serial resistance R_{sACp} and R_{sACs} of the primary and secondary

$$R_{sACp} = \frac{\rho_{cu} l_p}{w_p t_{eff}} \quad (13)$$

$$R_{sACs} = \frac{\rho_{cu} l_s}{w_s t_{eff}} \quad (14)$$

t_{eff} : is given by the expression; $t_{eff} = \delta(1 - e^{-(t/\delta)})$

3. Coupling capacitance C_{sp} and C_{ss} of the primary and secondary

$$C_{sp} = \frac{1}{2} \varepsilon_0 \varepsilon_{ox} \frac{t_p l_p}{s_p} \quad (15)$$

$$C_{ss} = \frac{1}{2} \varepsilon_0 \varepsilon_{ox} \frac{t_s l_s}{s_s} \quad (16)$$

Where, ε_0 is the permittivity of free space, $\varepsilon_0 = 8.854187.10^{-12} Mm^{-1}$.

4. Coupling capacitance C_{kps} between the primary and secondary, coupling capacitance C_{ksp} between the secondary and primary

$$C_{kps} = \varepsilon_0 \varepsilon_{ox} \frac{w l_p}{t_{ox}} \quad (17)$$

$$C_{ksp} = \varepsilon_0 \varepsilon_{ox} \frac{w l_s}{t_{ox}} \quad (18)$$

5. Oxide capacitance C_{oxp} and C_{oxs} of the primary and secondary

$$C_{oxp} = \frac{1}{2} l_p w_p \left(\frac{\varepsilon_0 \varepsilon_{ox}}{t_{ox}} \right) \quad (19)$$

$$C_{oxs} = \frac{1}{2} l_s w_s \left(\frac{\varepsilon_0 \varepsilon_{ox}}{t_{ox}} \right) \quad (20)$$

6. Resistances R_{subp} and R_{subs} associated to the silicon substrate of the primary and secondary

$$R_{subp} = 2\rho_{sub}\frac{t_{sub}}{l_p w_p} \quad (21)$$

$$R_{subs} = 2\rho_{sub}\frac{t_{sub}}{l_s w_s} \quad (22)$$

7. Capacitance C_{subp} and C_{subs} associated to the silicon substrate of the primary and secondary

$$C_{subp} = \tfrac{1}{2}\varepsilon_0\varepsilon_{sub}\frac{l_p w_p}{t_{sub}} \quad (23)$$

$$C_{subs} = \tfrac{1}{2}\varepsilon_0\varepsilon_{sub}\frac{l_p w_p}{t_{sub}} \quad (24)$$

Table III shows the electrical parameters calculated.

TABLE III. ELECTRICAL PARAMETERS RESULTS

Electrical parameters	Values
Primary inductance: L_p	49 nH
Secondary inductance: L_s	36 nH
Primary serial resistance: R_{sp}	0.21 Ω
Secondary serial resistance: R_{ss}	0.18 Ω
Primary serial resistance: R_{sACp}	0.48 Ω
Secondary serial resistance: R_{sACs}	0.42 Ω
Primary resistance of silicon substrate: R_{subp}	0.10 Ω
Secondary resistance of silicon substrate: R_{subs}	0.11 Ω
Primary coupling capacitance: C_{sp}	346.59 pF
Secondary coupling capacitance: C_{ss}	191.86 pF
Coupling capacitance between the primary and secondary: C_{kps}	44.83 pF
Coupling capacitance between the secondary and primary: C_{ksp}	38. 79 pF
Primary oxide capacitance: C_{oxp}	44.83 pF
Secondary oxide capacitance: C_{oxs}	38.79 pF
Primary capacitance of silicon substrate C_{subp}	38.79 pF
Secondary capacitance of silicon substrate : C_{subs}	33.56 pF
Quality factor Q_p	43.94
Quality factor Q_s	37.33

The quality factor is defined as the ratio between the magnetic power stored and the power dissipated in the component (29), (30). Thus, the higher the quality factor, the smaller the power lost in the component [11].

$$Q_p = \frac{\omega \mathrm{L_p}}{\mathrm{R_p}} \quad (25)$$

$$Q_s = \frac{\omega \mathrm{L_s}}{\mathrm{R_s}} \quad (26)$$

Figure 5 shows the evolution of the quality factor as a function of frequency for the primary and secondary winding.

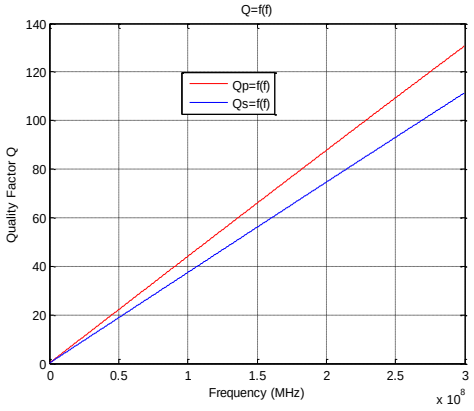

Fig. 5. Quality factor of the primary and secondary windings versus frequency

V. THE EFFICIENCY OF FLYBACK CONVERTER

The efficiency is calculated to see the performance of our Flyback converter [12-13].

$$\eta = \frac{P_{out} - P_{in}}{P_{out}} \quad (27)$$

$$P_{in} = P_j + P_f + P_{ed} \quad (28)$$

Transformer losses arise from [14-16]:

Winding joule losses: Current flowing through a winding's conductor causes joule heating. As frequency increases, skin effect and proximity effect causes the winding's resistance and, hence, losses to increase.

$$P_j = (R_{sp} + m^2 R_{ss}) I_{out}^2 \quad (29)$$

Hysteresis losses: Each time the magnetic field is reversed, a small amount of energy is lost due to hysteresis within the core.

$$P_f = m f^{\alpha} B_{\max}^{\beta} V \quad (30)$$

Where m, α *and* β are the coefficients depending on the size of the material. V is the volume of magnetic core.

Eddy current losses also called Foucault currents: Ferromagnetic materials are also good conductors and a core made from such a material also constitutes a single short-circuited turn throughout its entire length. Eddy currents therefore circulate within the core in a plane normal to the

flux, and are responsible for resistive heating of the core material.

$$P_{ed} = C\frac{f^2 B^2}{\rho} \qquad (31)$$

Where C and ρ are the coefficients depending on the size of the material.
The efficiency found is around 71%.

VI. THERMAL EFFECT IN A PLANAR MICRO-TRANSFORMER

In this section, we present the temperature distribution in our integrated micro-transformer, based on the finite element method [17-20].
This distribution is obtained by solving the equation (32) of heat taking into account certain boundary conditions.

$$\rho.C_p \frac{\partial T}{\partial t} - \nabla(k\nabla T) = q \qquad (32)$$

For an integrated micro-transformer in the air, the heat source can be expressed as (33)

$$q = \frac{P_{in}}{V} \qquad (33)$$

Where, V is the volume of our planar micro-transformer .
Geometry of this study is created in 3D space dimension. Our component consists of four domains. The domain of air surrounding our planar micro-transformer. The copper is the conductor material, the substrate is in ferrite, and the dielectric is in oxide.

In figure 6, we observe the temperature distribution in the planar micro-transformer on substrate. We see from these figures that the temperature is about 37 °C.

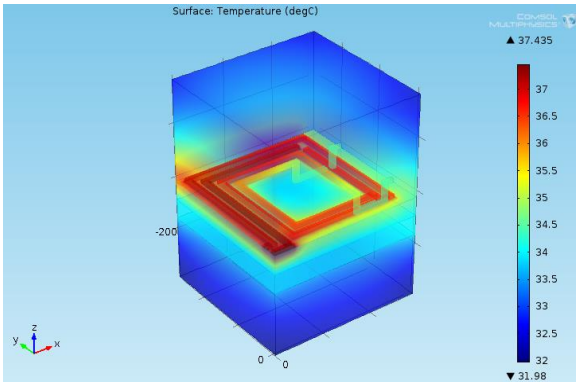

(a)

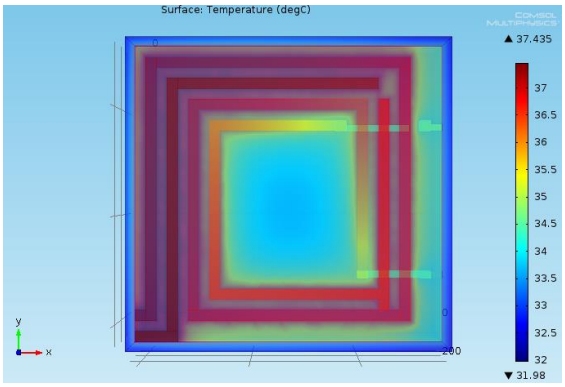

(b)

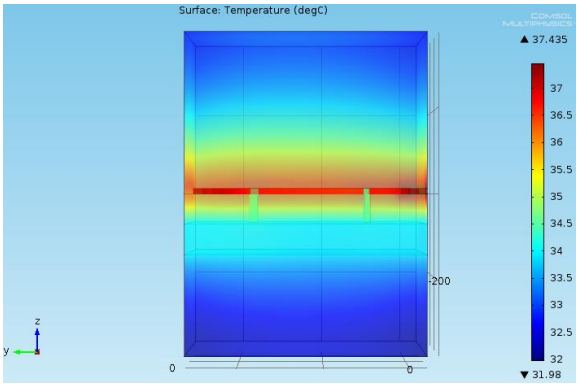

(c)

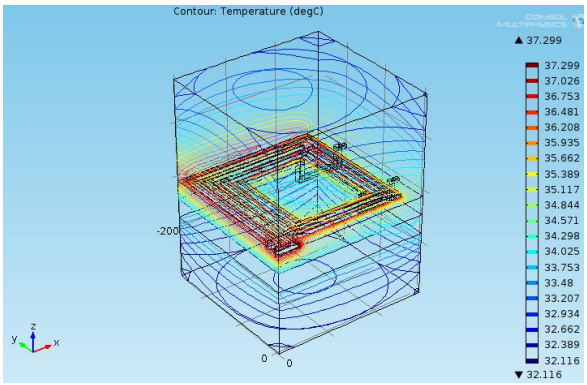

(d)

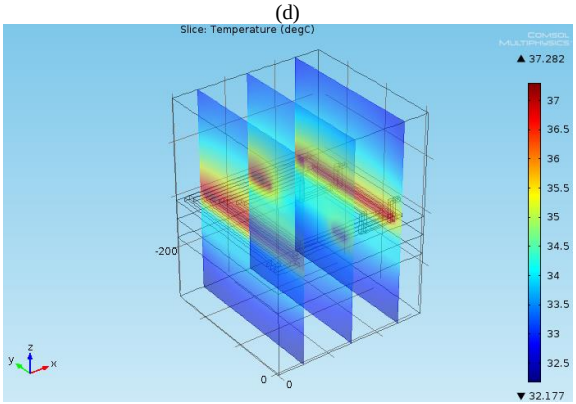

(e)

Fig. 6. Temperature distribution in the planar micro-transformer on substrate, (a) on general, (b) on dessu, (c) on front, (d) on contour, (e) on scile

VII. CONCLUSION

In this paper, design and analyze of a monolithic square spiral planar micro-transformer for its integration in a micro-converter has presented.

Higher efficiency of DC-DC Flyback using equivalent model parameters of transformer was obtained. The converter with the integrated transformer shows maximum efficiency of 71% for an output power 5 W.

We have visualized the thermal phenomenon in planar micro-transformer based on finite element method.

The simulation results show that an integrated planar micro transformer realized with substrate allows canalizing the magnetic field in the component. We conclude that the substrate losses can be minimized. It is also shown that the substrate of the monolithic component reduces losses also decreases the temperature.

ACKNOWLEDGMENT

Yamina Benhadda was born in Algeria in 1982. She obtained his Magister degree in plasma and electrical discharge at Mohamed Boudiaf University of Oran in 2010. She obtained his Doctorate degree in electrical engineering at Mohamed Boudiaf University of Sciences and Technology of Oran in 2016. In 2017, she became a full professor in this University. His research interests include the design and modeling of on-chip passive components, and the design of RF and millimeter-wave integrated circuits in silicon technologies. She is a member of research team of LEPA laboratory.

Mokhtaria Derkaoui is an associate professor, a PhD in electrical engineering and a young researcher in microelectronics from the University of Sciences and Technologies of Oran USTO, Algeria. She actually teaches modules in digital electronics and optoelectronics at the National Institute of Telecommunication & ICT of Oran INTTIC, Algeria. She is a member of research team of LEPA and LARATIC laboratories since 2010 and 2015 respectively.

Kheira Mendaz was born in Ain Temouchent (Algeria), on December 5, 1976. She graduated the University centre Belhadj Bouchaib, Electrical Engineering Department in Ain Temouchent (Algeria), in 2015. She received the Ph.D degrees in electrical engineering from Sidi Bel Abbes University, (Algeria), in 2015. She is Doctor at the University centre Belhadj Bouchaib, Electrical Engineering Department in Ain Temouchent (Algeria). His research interests concern: power electronics, electric machines, and EMC in power converter.

Hayet Kharbouch was born in Oran, Algeria. He received his PhD in 2018 from Mohamed Boudiaf University of Sciences and Technology of Oran.

REFERENCES

[1] M. Kim, F. Herrault, J. Kim and M. G. Allen, Monolithically-fabricated laminated inductors with electrodeposited silver windings, IEEE International Conference on Micro Electro Mechanical Systems (MEMS), pp. 873-876, Jan. 2013.

[2] J. Kim, J-. k. Kim, M. Kim, F. Herrault, M. G. Allen, Microfabrication of totoidal inductors integrated with nanolaminated ferromagnetic metallic cores, Journal of Micromechnics and Microengineering, 23(11), Nov. 2013.

[3] J. Kim, M. Kim, F. Herrault, J. Y. Park, and M. G. Allen, Electrodeposited nanolaminated CoNiFe cores for ultracompact DC-DC power conversion, IEEE Transactions on Power Electronics, 30(9), pp. 5078-5087, Sep. 2015.

[4] D. D. Yaya, M. B. Bechir, M. K. Youssouf, M. Soultan, F. Kahlouche, S. Capraro, A. Siblini, J. P. Chatelon and J. J. Rousseau, Characterization of integrated inductors with one and two YIG layers for low-power converters (1W), published by EDP Sciences, 2014.

[5] M. Derkaoui, A. Hamid, T. Lebey, R. Melati, Design and modeling of an integrated microtransformer in a flyback converter, Telkomnika, 11(4), pp. 669-682, 2013.

[6] S. Osmanaj, E. Nasufi, Design of an integrated planar inductor using accurate expressions for planar spiral inductances, IEEE Journal of Solid-State Circuits, 34(10), pp. 1419-1424, 1999.

[8] J. M. Wright, D. W. Lee, A. Mohan, A. Papou, P. Smeys, and S. X. Wang, Analysis of integrated solenoid inductor with closed magnetic core, IEEE Transactions on Magnetics, 46(6), pp. 2387-2390, Jun. 2010.

[9] C. R. Sullivan, D. V. Harburg, J. Qiu, C. G. Levey, and D. Yao, Integrating magnetic for on-chip power: a perspective, IEEE Transactions on Power Electronics, 28(9), pp. 4342-4353, Sep. 2013.

[10] H. Gan, On-chip transformer modeling, characterization, and applications in power and low noise amplifiers, These of Stanford University, March 2006.

[11] H. Yun, J. M. Kikkawa, J. Kim,T. Paik, C. R. Kagan, L. Meng, M. G. Allen, P. S. Jo, and C. B. Murray, Fabrication via a solution based process, Journal of Applied Physics 119, pp. 113901_1-113901_9, 2016.

[12] I. Aoki, Distributed active transformer-a new power-combining and impedance-transformation technique, IEEE Transactions on Microwave Theory and Techniques, 50(1), pp. 316-331, January 2002.

[13] I. Aoki, Fully integrated CMOS power amplifier design using the distributed active-transformer architecture, IEEE Journal of Solid-State Circuits, 37(3), pp. 371-383, March 2002.

[14] J. Muhlethaler, J. Biela, J. W. Kolar, and A. Ecklebe, Improved core-loss calculation for magnetic components employed in power electronic systems, IEEE Transactions on Power Electronics, 27(2), pp. 964-973, Feb 2012.

[15] P. Viarouge, J. C. Fagundes, E. Tourkhani, H. Le-Huy, Comportement thermique et conception des composants magnétiques dans les convertisseurs statiques de fréquence élevée, IEEE, pp. 582-585, 1995.

[16] C. Feeney, N. Wang, and S. C. O'Mathuna, A 20-MHz 1.8-W DC-DC converter with parallel microinductors and improved light-load efficiency, IEEE Transactions on Power Electronics, 30(2), pp. 771-779, Jan 2015.

[17] Y. Benhadda, A. Hamid, T. Lebey, M. Derkaoui, Design and modeling of an integrated inductor in a buck converter DC-DC, Journal of Nano and Electronic Physics, 7(2), pp. 2006 (6pp), 2015.

[18] A. Allaoui, A. Hamid, P. Spiterri, V. bley, T. Lebey, Thermal modeling of an integrated inductor in a micro-converter, Journal of Low Power Electronics, 11(1), pp. 63-73, 2015.

[19] Y. Benhadda, A. Hamid, T. Lebey, A. Allaoui, M. Derkaoui, R. Melati, Thermal behavior of an integrated square spiral micro coil, Telkomnika, 14(2), pp. 669-682, 2015.

[20] Y. Benhadda, A. Hamid, T. Lebey, Dimensioning and Modeling of a Circular Inductor Integrated in a Boost Converter, Journal of Nano and Electronic Physics, 8(4), 04039 (5pp), 2016.